Rhabdomere biogenesis in *Drosophila* photoreceptors is acutely sensitive to phosphatidic acid levels

Padinjat Raghu,[1] Elise Coessens,[1,3] Maria Manifava,[1] Plamen Georgiev,[1] Trevor Pettitt,[1] Eleanor Wood,[1] Isaac Garcia-Murillas,[1] Hanneke Okkenhaug,[1] Deepti Trivedi,[1] Qifeng Zhang,[1] Azam Razzaq,[2,4] Ola Zaid,[1] Michael Wakelam,[1] Cahir J O'Kane,[2] and Nicholas Ktistakis[1]

[1]Inositide Laboratory, Babraham Institute, Babraham Research Campus, Cambridge CB22 3AT, England, UK
[2]Department of Genetics, University of Cambridge, Cambridge CB2 3EH, England, UK
[3]Institut de Biologie du Developpement de Marseille Luminy, 13288 Marseille, Cedex 09, France
[4]Avecia, Billingham TS23 1YN, England, UK

Phosphatidic acid (PA) is postulated to have both structural and signaling functions during membrane dynamics in animal cells. In this study, we show that before a critical time period during rhabdomere biogenesis in *Drosophila melanogaster* photoreceptors, elevated levels of PA disrupt membrane transport to the apical domain. Lipidomic analysis shows that this effect is associated with an increase in the abundance of a single, relatively minor molecular species of PA. These transport defects are dependent on the activation state of Arf1. Transport defects via PA generated by phospholipase D require the activity of type I phosphatidylinositol (PI) 4 phosphate 5 kinase, are phenocopied by knockdown of PI 4 kinase, and are associated with normal endoplasmic reticulum to Golgi transport. We propose that PA levels are critical for apical membrane transport events required for rhabdomere biogenesis.

Introduction

During development, eukaryotic cells undergo morphogenetic changes to suit ongoing physiological needs. Effecting cell shape changes involves complex cell biological processes, including changes in both the cell membrane and the cytoskeletal. An essential element of membrane biogenesis is the need to achieve regulated vesicular transport such that membranes can be delivered to the desired domain of the cell. This process is thought to involve a complex interplay of the physical properties of the lipid constituents in membranes as well as the activities of proteins that can affect membrane curvature. Conceptually, the lipid constituents of the cell membranes could be those with essentially structural roles (such as phosphatidylcholine [PC], phosphatidylethanolamine, phosphatidylserine (PS), and cholesterol) and signaling lipids whose levels change in a regulated manner. These signaling lipids include DAG, its phosphorylated derivative phosphatidic acid (PA), and several phosphorylated species of phosphatidylinositol (PI).

In the simple eukaryote *Saccharomyces cerevisiae* that recapitulates most basal transport pathways conserved in higher eukaryotes, genetic analysis has implicated several lipids in regulating membrane traffic. Evidence showing that DAG and PA can affect membrane transport comes from yeast through analysis of *SEC14*, a gene that encodes a PI/PC transfer protein essential for viability and transport from the Golgi (Bankaitis et al., 1990). The sec14 phenotype can be suppressed/bypassed by mutants in several genes that control biosynthesis of PI and PC (Cleves et al., 1991). However, the ability of such mutants to bypass sec14 has an obligate requirement for *SPO14* that encodes phospholipase D (PLD; Xie et al., 1998), an enzyme that generates PA from PC. Although Spo14p is not required for vegetative growth (Sreenivas et al., 1998; Xie et al., 1998), it is

The Rockefeller University Press $30.00
J. Cell Biol. Vol. 185 No. 1   129–145
www.jcb.org/cgi/doi/10.1083/jcb.200807027

JCB   **129**

required to form the prospore membrane (Rudge et al., 1998) and for PA synthesis during sporulation (Rudge et al., 2001); loss of Spo14p leads to accumulation of undocked prospore membrane precursors vesicles on the spindle pole body (Nakanishi et al., 2006). Thus, in yeast, PA generated by Spo14p activity plays a key role in this membrane trafficking event. Although the analysis of spo14 has implicated PA and its downstream lipid metabolites in membrane transport, to date there is little direct evidence to suggest that PA can function as a regulator of membrane traffic in metazoans. The idea that PA can function in a signaling capacity during membrane transport has been fueled by the observations that (a) in vitro ADP ribosylation factor (Arf) proteins, key mediators of membrane transport, can regulate the activity of PLD (Brown et al., 1993; Cockcroft et al., 1994), (b) overexpression of PLD in several different cell types affects processes likely to require exocytosis (Vitale et al., 2001; Choi et al., 2002; Cockcroft et al., 2002; Huang et al., 2005), and (c) overexpression of mammalian PLD1 is reported to promote generation of β–amyloid precursor protein-containing vesicles from the TGN (Cai et al., 2006). However, the role of PA in regulating secretion in these settings remains unclear, and currently, there is little evidence linking demonstrable changes in PA levels with the molecular machinery that regulates membrane traffic in vivo.

In this study, we have used *Drosophila melanogaster* photoreceptors as a model system to test the effect of altered PA levels on membrane traffic. We show that elevated levels of PA disrupt membrane transport to the apical domain of photoreceptors with defects in the endomembrane system.

Results

Elevated PA levels result in defective rhabdomere biogenesis

Sensory transduction in *Drosophila* photoreceptors occurs in a specialized compartment, the rhabdomere (Hardie and Raghu, 2001). Photoreceptors are polarized cells, and the rhabdomere is the expanded apical domain of these cells, consisting of 30,000 microvilli (Fig. 1, A and B; Hardie and Raghu, 2001). The plasma membrane of the rhabdomere contributes ∼90% of the membrane surface area of photoreceptors (Leonard et al., 1992); its growth is triggered during the last 30% of pupal development (pd) by a process of intense membrane biogenesis and polarized vesicle trafficking.

We tested the effect of increased PA levels on rhabdomere biogenesis by exploiting a loss of function mutant in cytidine diphosphate (CDP)–DAG synthase, an enzyme that condenses PA with CTP to produce CDP-DAG (Fig. 1 C; Heacock and Agranoff, 1997). This reaction is the first step in the synthesis of PI, phosphatidylglycerol (PG), and cardiolipin, and in principle, a reduction of CDP-DAG activity should result in accumulation of PA. A single gene encodes CDP-DAG synthase activity in *Drosophila* (*cds*). For this study, we used *cds[1]*, a severe hypomorph in this gene (Wu et al., 1995). In photoreceptors, a major source of PA is the phototransduction cascade, where it is generated by the sequential activity of phospholipase Cβ (PLC) and diacylglycerol kinase (DGK; Fig. 1 C).

cds[1] photoreceptors show light-dependent retinal degeneration that can be rescued by dark rearing or by blocking light-induced PLC activity (Wu et al., 1995). During this study, we grew *cds[1]* flies in bright light to trigger PA accumulation and examined the photoreceptors by transmission EM (TEM). As previously reported (Wu et al., 1995), when grown in constant light, *cds[1]* photoreceptors showed vesiculation and a variable reduction in the size of the rhabdomeres (Fig. 2 B). In addition, and more significantly for the purpose of this study, we observed that the cell body of *cds[1]* photoreceptors showed the presence of abnormal expanded endomembranes (Fig. 2 B, v). In some instances, these apparently tubular organelles appeared studded with electron-dense structures resembling ribosomes (Fig. 2 C). These ultrastructural changes were associated with specific molecular defects. The level of rhodopsin 1 (Rh1), a major rhabdomeral protein, was dramatically reduced (Fig. 2 J). We found that the levels of two other rhabdomeral proteins, TRP (Montell and Rubin, 1989; Hardie and Minke, 1992) and NORPA (Schneuwly et al., 1991), were also reduced (unpublished data). Our findings demonstrate that in the *cds[1]* mutant, there are defects in the apical rhabdomere membranes, accumulation of abnormal endomembranes in the cell body, and changes in the levels of rhabdomeral proteins.

The phenotypes of the loss of function *cds[1]* mutant could result from accumulation of PA or a reduction in the levels of phospholipids such as PI, PG, and cardiolipin whose biosynthesis requires the activity of CDP-DAG synthase (Fig. 1 C). Lipidomic analysis of *cds[1]* retinae revealed reductions in the levels of some molecular species of PI, PG, and PS (unpublished data). To distinguish between these possibilities, we analyzed the effect of increasing PA levels using two further manipulations: (1) overexpression of *Pld* and (2) overexpression of DGK (Fig. 1 C). The *Drosophila* genome contains a single gene (*Pld*) encoding a PLD-like protein (Lalonde et al., 2005). We obtained a full-length cDNA clone for this gene and showed that it expressed a functional PLD activity (Fig. S1). When *Pld* is expressed in photoreceptors, it localizes to a subcompartment of the cell body at the base of the rhabdomeres (Fig. S5 A), and colocalization experiments with Rh1 (a protein restricted to the rhabdomere) showed that PLD does not localize to the apical domain (Fig. S5 C). TEM analysis of photoreceptors overexpressing *Pld* revealed vesiculation of the rhabdomeres and degeneration (Fig. 2 E) similar to but much stronger than in *cds[1]*. In addition, the cell body showed accumulation of expanded tubulovesicular membranous structures. In the most extreme cases, these appeared as concentric stacks of membranes (Fig. 2 G). These ultrastructural changes were accompanied by molecular changes similar to those observed in *cds[1]*. Western blot analysis showed reduced levels of Rh1, TRP, and NORPA (Fig. 2 I). These phenotypes were not observed (Fig. 2 F) in flies overexpressing equivalent levels of a demonstrated (Fig. S1 C) catalytically dead construct (K/R mutant, lysine 1086 changed to arginine) of *Pld*. Collectively, these findings show that when overexpressed, catalytically active PLD generates a metabolite that causes ultrastructural and molecular changes reminiscent of those seen in *cds[1]* loss of function mutants.
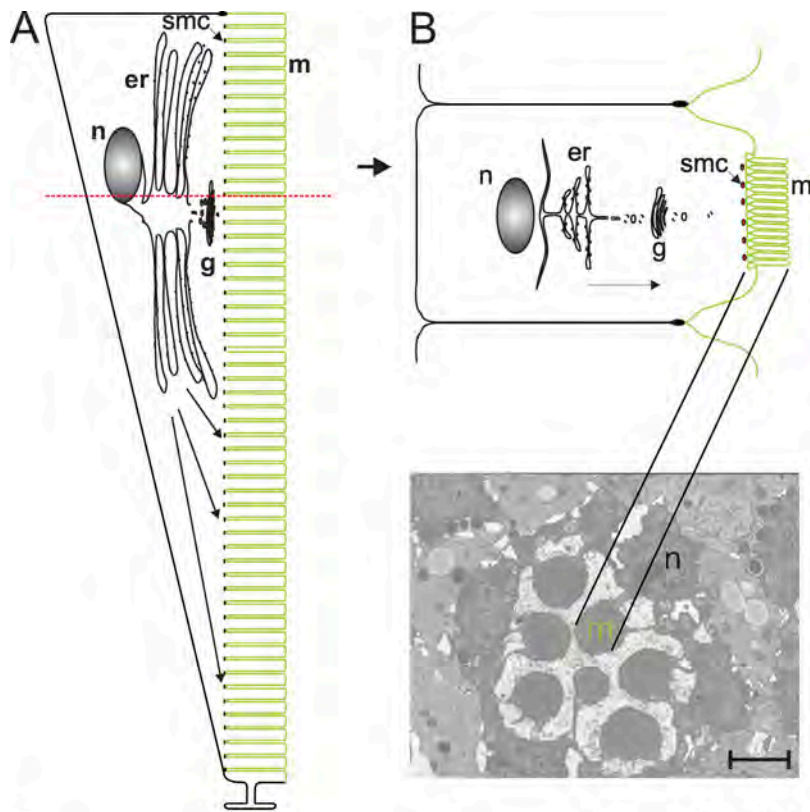
Figure 1. *Drosophila* **photoreceptor structure.** (A) Longitudinal section through a single photoreceptor showing the relationship of the cell body and rhabdomeres composed of microvilli (m). Organelles located in the cell body are shown. The submicrovillar cisternae (smc) are shown at the junction of the cell body and the rhabdomere. The rhabdomeral plasma membrane is shown in green. The red dotted line shows the level of the cross section in B. n, nucleus; g, Golgi. (B) Cross section through a photoreceptor at the level of the nucleus showing the organelles. The arrow marks the direction of polarized transport to the apical domain. A representative TEM from a wild-type ommatidium is shown with the microvilli and nucleus marked. Bar, 2 μm. (C) Metabolic fates of PA. In addition to de novo biosynthesis from fatty acids and glycerol, PA can be generated by the sequential activity of PLC and DGK or by hydrolysis of PC by PLD. PA can undergo four metabolic fates: (1) allosteric activation of PA-binding proteins, (2) dephosphorylation to DAG by LPP, (3) generation of lyso-PA by phospholipase A_2 (PLA$_2$), and (4) condensation with CTP by CDP-DAG synthase (CDS) to generate CDP-DAG, a precursor for the biosynthesis of PI, PG, and cardiolipin. PI4P, PI 4-phosphate; SKTL, PI 4-phosphate 5 kinase.
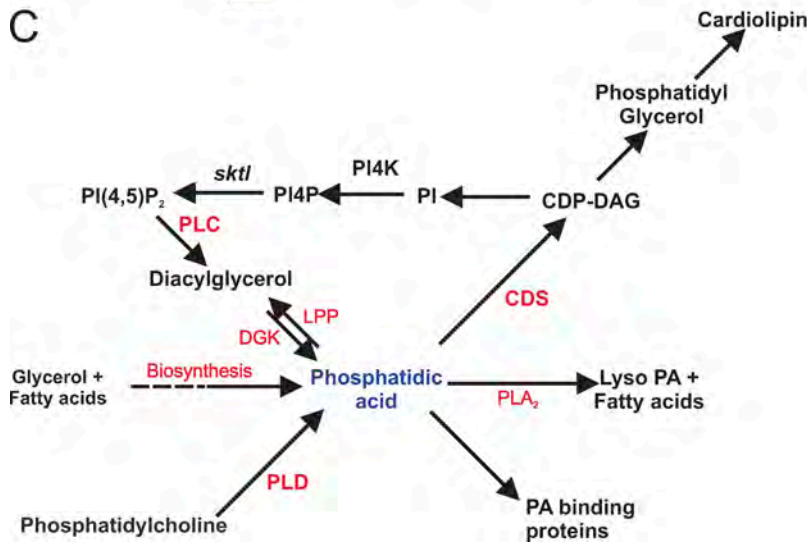
Finally, we also tested the effect of overexpressing DGK encoded by the *rdgA* gene (Masai et al., 1993). This resulted in the accumulation of a large number of tubular and vesicular transport intermediates within the cell body (Fig. 2 H). Such structures were not seen in control photoreceptors (Fig. 2 D). Because increased levels of PA are the immediate common biochemical outcome of all three genetic manipulations, our findings strongly suggest that in vivo, elevated levels of PA are able to perturb endomembrane homeostasis in photoreceptors.

To test whether increased levels of PA are associated with this phenotype, we measured the levels of this lipid in retinal extracts from *cds*[1], *Pld*, and *rdgA* overexpressing retinae using liquid chromatography followed by mass spectrometry.

These experiments revealed no significant elevation in total retinal PA levels (unpublished data). However, because total PA includes contributions from a larger biosynthetic pool as well as a smaller signaling pool, we examined the abundance of ∼20 individual species of PA that can be separately quantified by liquid chromatography mass spectrometry. In the case of *cds*[1], we found a significant elevation of a single species of PA (predicted fatty acyl composition 16:0/18:2, also called 34:2) relative to controls (Fig. 3 A). Remarkably, when *Pld* was overexpressed, a smaller elevation of the same species of PA was seen relative to both wild-type (no overexpression) as well as the overexpression of catalytically dead PLD (Fig. 3 B). Finally, in retinae overexpressing *rdgA*, an
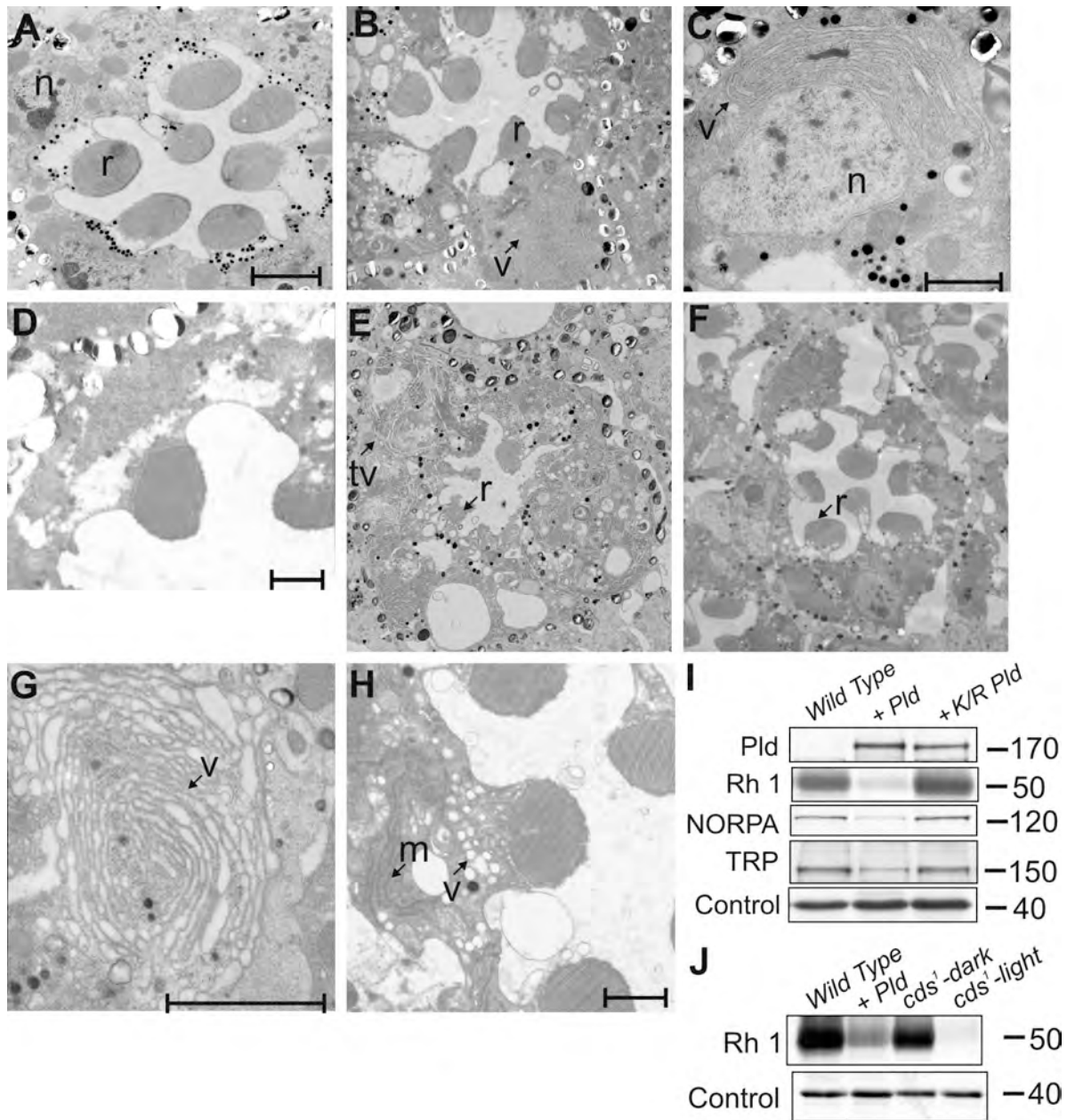
Figure 2. **Endomembrane defects in photoreceptors with elevated PA levels.** (A and B) TEM showing the ultrastructure of an ommatidium from wild-type eye cds^1 (A) grown in bright light (B). (C) Higher magnification showing abnormal endomembrane accumulations (v) in the cell body of cds^1. (E and F) Rhabdomere (r) degeneration and membranous structures (tv) seen when wild-type (E) but not K/R Pld (F) is expressed in photoreceptors. (G) High magnification view of expanded endomembrane structures. (H) Overexpression of $rdgA$ causes accumulation of membranous and vesicular transport intermediates in the cell body. (D) GMR-GAL4 alone is normal. (I) Western blots showing expression of equivalent levels of wild-type and K/R Pld. The reductions in the levels of Rh1, NORPA, and TRP are seen only when wild-type Pld is overexpressed. (J) Western blot showing reduced levels of Rh1 in flies overexpressing Pld and cds^1. Wild-type flies and cds^1 grown in the dark are shown as controls. Control band shows equivalent levels of protein loading. n, nucleus; m, membranous transport intermediate. (I and J) Unit of measure, M_r. Bars: (A, D, and H) 2 µm; (C and G) 1 µm.

elevation in 16:0/18:2 PA was also seen (Fig. 3 C). The acyl chain composition of this species reflects that of the most abundant species of PI and PC in *Drosophila* retinal lipid extracts (unpublished data). PI and PC are the substrates from which PA is generated by PLC (in cds^1 grown in bright light to trigger PA accumulation) and PLD (Pld overexpression), respectively. The levels of PC, DAG, and PI were not altered in retinae from these genotypes (Fig. 3, D–F). Our findings demonstrate a common biochemical basis, namely elevation in the

abundance of a single molecular species of PA, for the endomembrane defects described in this study.

To further test the role of PA in the phenotypes described, we attempted to reverse the phenotypes of Pld overexpression or cds^1 by coexpressing a type II PA phosphatase, lipid phosphate phosphohydrolase (LPP; Fig. 1 C; Garcia-Murillas et al., 2006). The effect of LPP was analyzed using a combination of TEM and Western blots for Rh1 levels. These analyses revealed that LPP could substantially reverse the reduction of Rh1 levels
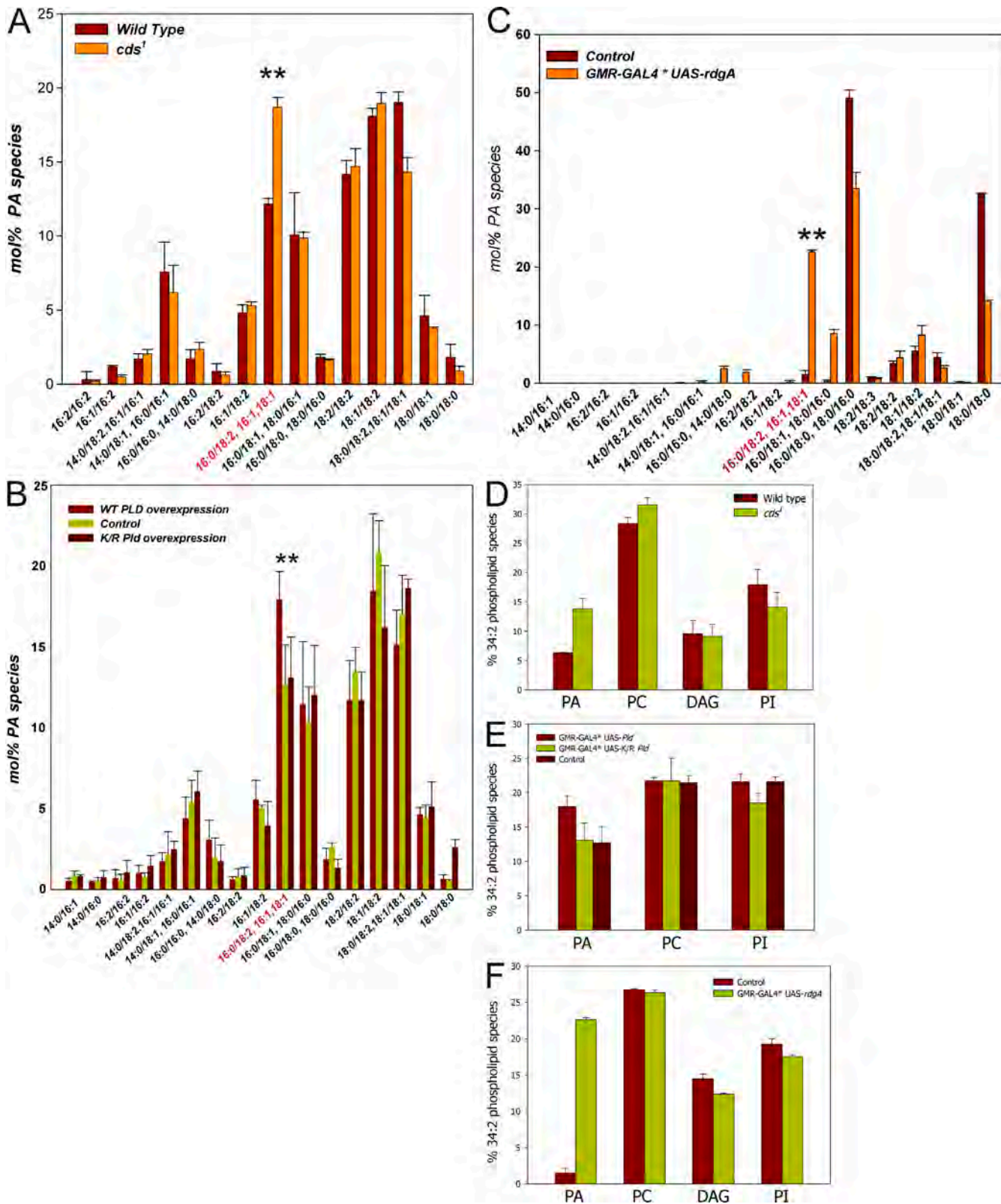
Figure 3. **Lipidomic analysis of changes in PA and other phospholipids.** Analysis of PA levels in photoreceptors by mass spectrometry. The acyl chain composition of each species predicted from its M_r is shown on the x axis. The y axis shows the abundance of each species as a percent of total PA in that sample. (A–C) Elevation of 16:0/18:2 PA in cds^1 relative to wild type (A), in flies overexpressing Pld but not K/R Pld or controls (B), and in flies overexpressing $rdgA$ (C). The elevated species is marked in red on the x axis and is indicated by **. Levels of PC, DAG, and PI were measured from retinae of the following three genotypes: cds^1 (D), Pld overexpression (E), and $rdgA$ (F). Error bars indicate mean ± SD of the 34:2 species of each phospholipid.
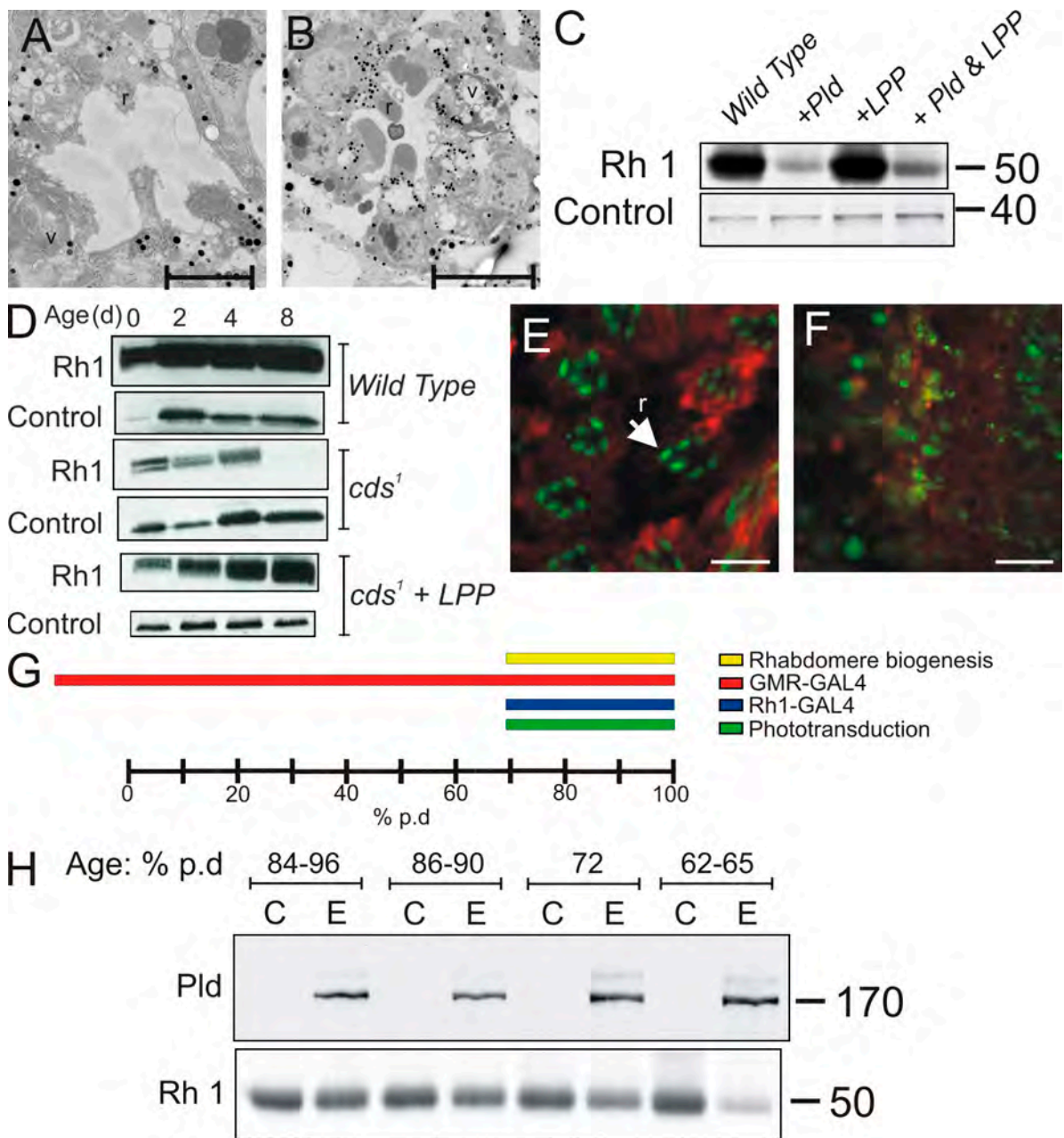
Figure 4. **Reversal of PA effects by expression of a type II PA phosphatase.** (A and B) TEM analysis of photoreceptors overexpressing *Pld* alone (A) and *Pld* and LPP (B). Rhabdomeres (r) and membranous structures (v) are shown. Bars, 5 µm. (C) Western blots comparing the levels of Rh1 protein in the specified genotypes. Control bands show equivalent levels of protein loading. (D) Rh1 levels in *cds¹* mutants grown in 4 h light/20 h dark illumination cycles compared with *cds¹*-coexpressing LPP. Samples from flies 0-, 2-, 4-, and 8-d-old are shown. Levels in wild-type flies are also shown. Levels of syntaxin are used as a loading control. (E and F) Immunofluorescence labeling of photoreceptors expressing wild-type (F) or K/R *Pld* (E). Rhabdomeres where the subcellular localization of Rh1 is normally restricted are shown in green in E; ER is labeled in red with an antibody to the KDEL epitope. In photoreceptors expressing *Pld*, Rh1 signals are no longer restricted to the rhabdomere but are distributed through the cell body. A critical time window for the effects of PLD overexpression. Bars, 10 µm. (G) Diagrammatic representation of the course of *Drosophila* pd. Time axis is shown as a percent of pd. In our conditions, this is 100 h. The temporal expression patterns Rh1-GAL4 and GMR-GAL4 are shown. The time of onset of phototransduction is also shown along with the duration of the rapid last phase of rhabdomere biogenesis. (H) Western blots from head extracts of control and experimental animals in which expression of *Pld* had been induced using heat shock GAL4 at the age specified (% pd). Animals not expressing *Pld* are marked as C, and those with *Pld* overexpression are marked as E. (top) Levels of *Pld* detected using a polyclonal antibody to this protein are shown. (bottom) Levels of Rh1 detected using a monoclonal antibody to this protein are shown. In the case of *cds¹*, in which the elevation of PA is generated by sequential light-activated PLC and DGK, PA accumulation most likely starts at ∼70% pd when Rh1 and associated transduction components are first expressed, making the cell phototransduction competent. (H) Unit of measure, *M*r.

in *cds¹* mutant (Fig. 4 D) grown in light (4 h light/20 h darkness). In the case of *Pld* overexpression, coexpression of LPP could only reverse the reduction in Rh1 levels to a limited extent

(Fig. 4 C). This partial rescue was reflected in TEM analysis of retinal ultrastructure (Fig. 4, compare A with B). Although significant rescue of rhabdomeral degeneration could be seen,

every ommatidium still showed 2–3 degenerate rhabdomeres, and some abnormal endomembrane structures could be seen (Fig. 4 B) in the cell body.

A critical developmental time window for the effect of elevated PA levels

During our experiments, we observed that *Pld* overexpression in photoreceptors using glass multimer reporter (GMR)–GAL4 and Rh1-GAL4 had different outcomes. When expression in photoreceptors was performed during late pd (>72% pd) using Rh1-GAL4, there appeared to be no ultrastructural or molecular phenotypes (unpublished data) at eclosion. In contrast, overexpression using GMR-GAL4 resulted in the strong phenotypes described in Fig. 2 E. Because equivalent levels of PLD protein are expressed using these two drivers, one possible explanation was that the distinct temporal expression patterns obtained using GMR-GAL4 and Rh1-GAL4 (Fig. 4 G) result in differing outcomes. To test this idea, we induced *Pld* overexpression in photoreceptors at defined points of time during pd using heat shock GAL4 and assayed its effect using Western blots for Rh1 levels. This analysis revealed that to observe the reduction in Rh1 levels characteristic of *Pld* overexpression (Fig. 2 I), it was necessary to express *Pld* at or before 70% pd (Fig. 4 H). Expression of *Pld* after this time point gave no reduction in Rh1 levels; expression at 70% pd gave a marginal reduction, whereas expression at 62–65% pd gave the characteristic reduction in Rh1 levels (Fig. 4 H). These findings suggest a critical time window during pd before which PA levels in photoreceptors have a profound impact on rhabdomere biogenesis.

Enhanced activity of Arf1 but not Arf6 mediates the effects of elevated PA levels

To understand the mechanism by which elevated PA disrupts rhabdomere biogenesis, we modulated the activity of two members of the Arf family of small GTPases that play a key role in the organization of secretory and endocytic membrane traffic (D'Souza-Schorey and Chavrier, 2006; Gillingham and Munro, 2007). Arf1 is thought to regulate the assembly of coat complexes along the early secretory pathway, notably between ER and Golgi, between the Golgi cisternae and at the trans-Golgi, whereas Arf6 is thought to regulate endosomal traffic at the plasma membrane. To alter the activity of Arf1 (class I Arf), we overexpressed the guanine nucleotide exchange factor (GEF) that is expected to enhance levels of active Arf1-GTP (Fig. 5 G). In *Drosophila*, the *garz* gene (Kraut et al., 2001) encodes a protein with homology to the mammalian Arf1-GEF Golgi-specific brefeldin resistance factor (Cox et al., 2004). To overexpress *garz* in photoreceptors, we used an enhancer promoter line inserted upstream of the *garz* gene that allows overexpression of endogenous *garz* using the GAL4/upstream activation sequence (UAS) system (Rorth, 1996). We overexpressed *garz* in developing photoreceptors using GMR-GAL4. TEM analysis revealed that overexpression of *garz* results in normal rhabdomere development with no abnormal accumulation of endomembranes in the cell body (Fig. 5 C). To test the consequence of enhanced Arf1 activity on photoreceptors with elevated PA levels, we overexpressed *garz* along with *Pld*. This resulted in a massive enhancement of the phenotype seen by overexpressing *Pld* alone (Fig. 5, compare C with E). In any given retina, we could at best detect one or two poorly developed rhabdomeres; apart from this, there was virtually no development of rhabdomeres. To test whether this was a direct consequence of enhanced Arf1 activity, we tested the effects of overexpressing the GTPase-activating protein (GAP) for Arf1. Arf1-GAP is expected to enhance the hydrolysis of GTP on GTP-Arf1 to GDP-Arf1, thereby reducing Arf1 activity (Fig. 5 G). To do this, we generated transgenic flies expressing *Drosophila* Arf1-GAP (dArf1-GAP), which is encoded by the gene *Gap69C* (Frolov and Alatortsev, 2001). When overexpressed in wild-type photoreceptors using the GAL4/UAS system, dArf1-GAP results in a mild rough eye phenotype. TEM revealed that rhabdomeres developed normally, and there were at best mild endomembrane defects in the cell body (Fig. 5 D). To examine the effect of reducing Arf1-GTP levels in photoreceptors with elevated PA levels, we coexpressed dArf1-GAP and *Pld*. This resulted in a substantial but incomplete rescue of rhabdomere size compared with flies overexpressing *Pld* alone (Fig. 5, compare D with F).

We also tested the effects of altering Arf1 activity in cds^1 photoreceptors. Because PA accumulation in cds^1 is triggered in bright light illumination, we performed experiments under these conditions. In contrast to flies grown in the dark, overexpression of *garz* and dArf1-GAP in wild-type photoreceptors grown in bright light resulted in some defects in rhabdomere structure and mild accumulation of endomembranes (Fig. 6, A and C). When *garz* was overexpressed in cds^1, rhabdomere size and structure were significantly worse (Fig. 6 B) than in *garz* alone (Fig. 6 A) or cds^1 alone (Fig. 2 B). Overexpression of dArf1-GAP in cds^1 resulted in a dramatic increase in the accumulation of whorls of endomembrane within the cell body (Fig. 6 D) accompanied by the appearance of poorly formed rhabdomeres. Collectively, these observations strongly suggest that the endomembrane defects observed in photoreceptors with elevated PA levels (both cds^1 and *Pld* overexpression) occur in the context of ongoing Arf1 activity.

We also tested the consequence of altering Arf6 activity on photoreceptors with elevated PA. To enhance the activity of Arf6, we overexpressed *schizo* (Onel et al., 2004), which encodes a *Drosophila* SEC7 domain containing protein with greatest homology to mammalian EFA6 (Perletti et al., 1997; Franco et al., 1999) and Arf-GEF100 (Someya et al., 2001). This manipulation is expected to enhance the levels of active Arf6-GTP (Fig. 7 A). When *schizo* was overexpressed in wild-type photoreceptors, rhabdomere biogenesis was largely unaffected with minimal endomembrane defects (Fig. 7 E). However, when *schizo* was coexpressed with *Pld,* this did not result in an enhancement of the phenotypes of overexpressing *Pld* alone (Fig. 7, compare F with G). Conversely, we also overexpressed *Pld* in a loss of function mutant of the only *Drosophila* Arf6 gene (Fig. S4). By TEM analysis, this Arf6 mutant showed normal photoreceptor ultrastructure (Fig. 7 C), and overexpression of *Pld* in this background was just as effective as expressing it in wild-type photoreceptors. Collectively, these results strongly suggest that the endomembrane defects observed in photoreceptors with elevated PA levels are not mediated by changes in Arf6 activity.
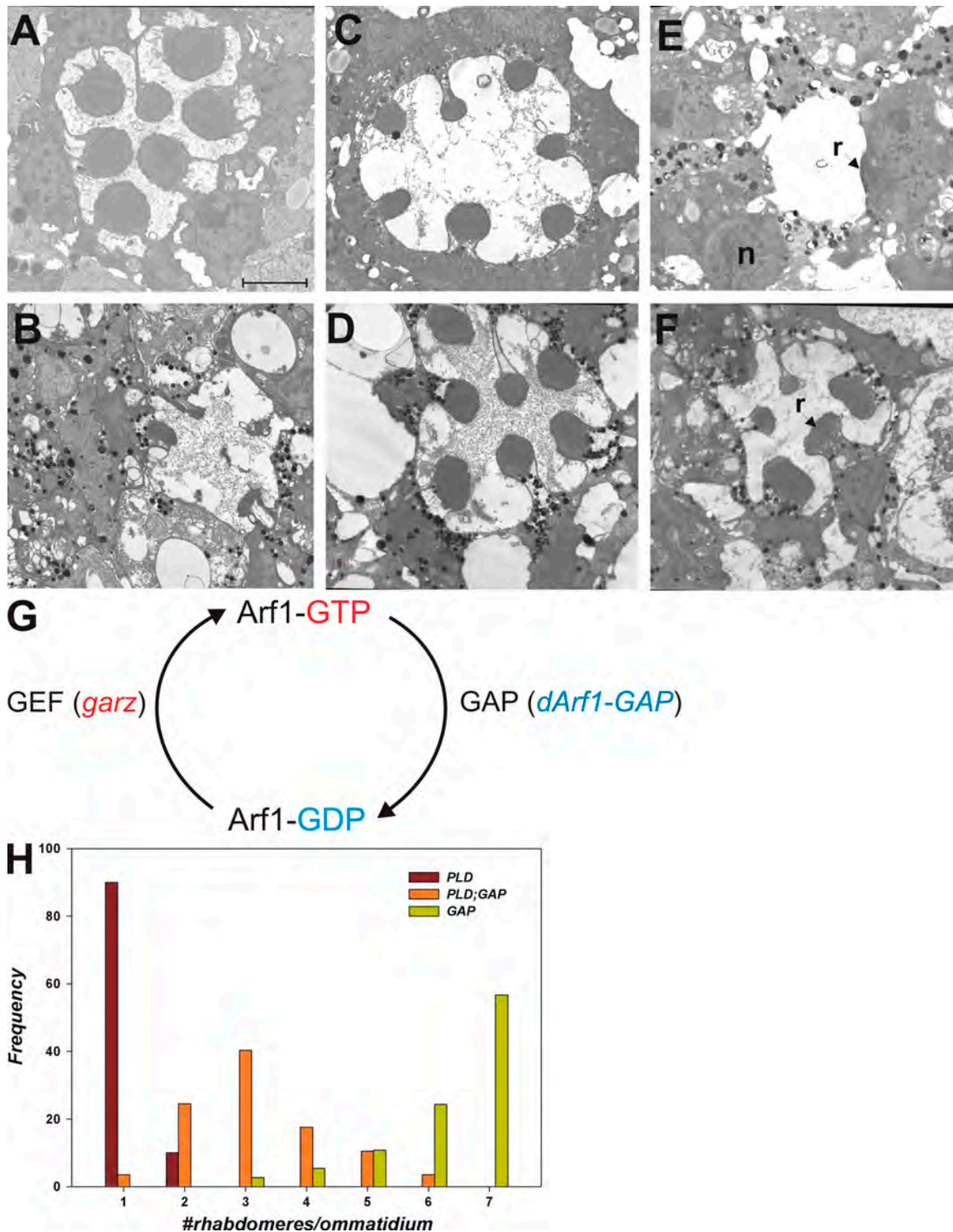
Figure 5. **Effects of *Pld* overexpression in photoreceptors with altered Arf1 activity.** TEM analysis of photoreceptors. (A–C and E) Wild-type (A) over-expressing *Pld* (B), *garz* (C), and *Pld* and *garz* together (E). (G) Representation of the activity states of Arf1 and the enzymes that convert Arf1 between these states. Arf1-GTP, GTP-bound Arf1; Arf1-GDP, GDP-bound Arf1. (D and F) TEM analysis of photoreceptors overexpressing *dArf1-GAP Pld* (D) and *dArf1-GAP* (F). (H) Quantitative analysis of rhabdomere biogenesis defects. Genotypes are marked. The x axis shows bins for ommatidia with a given number of rhabdomeres developed. The y axis shows frequency of rhabdomeres falling within a given bin for each of the genotypes. At least 50 ommatidia were analyzed from three separate heads. r, rhabdomere; n, nuclei. Bar, 2 μm.

Reduced α-adaptin function does not suppress the effects of *Pld* overexpression

To reduce endocytosis at the plasma membrane, we targeted α-adaptin, a specific subunit of the AP-2 complex. The AP-2 complex is found at the plasma membrane and is not known to have a function at the TGN or endosomes (Robinson, 2004). Because null mutants in the only *Drosophila* gene-encoding α-adaptin (CG4260) are homozygous lethal during embryonic development
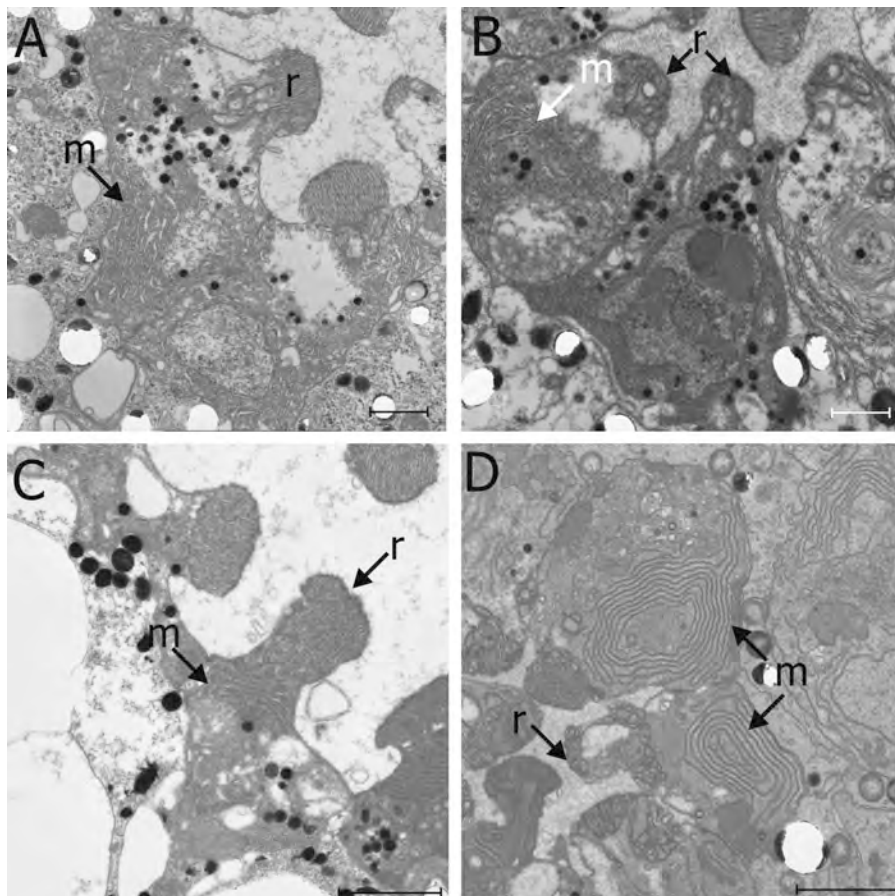
Figure 6. **TEM analysis of the effects of Arf1 modulation in *cds¹* photoreceptors.** (A) Overexpression of *garz* in flies grown in bright light illumination. Variable effects on rhabdomeres (r) are seen, and some accumulation of membranes (m) is also observed. (B) Overexpression of *garz* in *cds¹* results in a substantial worsening of rhabdomeres but no changes in the accumulation of membranes. (C) Overexpression of dArf1-GAP in flies grown in bright light illumination has a clear but minimal effect on rhabdomeres and some accumulation of membranes in the cell body. (D) Overexpression of dArf1-GAP results in a massive accumulation of membranes in the cell body and a worsening of the rhabdomere biogenesis effects. Bars: (A–C) 1 μm; (D) 2 μm.

(Gonzalez-Gaitan and Jackle, 1997), we disrupted its function specifically in the eye by transgenic RNAi knockdown using GMR-GAL4 (Dietzl et al., 2007). Three independent RNAi lines for α-adaptin were used with essentially similar results. Data are presented for one of the lines.

When α-adaptin function is reduced by GMR-GAL4* UAS-RNAi[α-adaptin], rhabdomere biogenesis is disrupted. Individual rhabdomeres (Fig. 8, r) are smaller and ill formed (Fig. 8 H), the base of the rhabdomeres is distorted, and the cell bodies show accumulation of membranous structures (Fig. 8, m). We coexpressed *Pld* and UAS-RNAi[α-adaptin] using GMR-GAL4. TEM analysis revealed that retinae from such animals have virtually no detectable rhabdomeres (Fig. 8 I). The cell bodies of the photoreceptors from such animals continued to show accumulation of membrane transport intermediates (Fig. 8, m). These results strongly suggest that reducing the function of AP-2 complexes cannot suppress the transport defects seen as a result of elevated PA levels.

Reduced dynamin activity enhances the effects of *Pld* overexpression

We tested the effect of reducing dynamin function on the phenotypes arising from *Pld* overexpression. To do this, we exploited a temperature-sensitive allele of *shibire* (*shi¹*) that encodes *Drosophila* dynamin (Kosaka and Ikeda, 1983; van der Bliek and Meyerowitz, 1991). *shi¹* shows wild-type dynamin activity at 18°C and behaves as a loss of function at 29°C. Because *shi¹*

shows pupal lethality when grown at 29°C and our experiments of the effects of *Pld* overexpression required dynamin function to be restricted during late pd, we grew flies at 23°C, which allows *shi¹* to eclose as adults with a partial loss of dynamin function (Alloway et al., 2000; Kiselev et al., 2000). When *Pld* is overexpressed in photoreceptors of flies grown at 23°C, all of the endomembrane defects described when overexpression is performed at 25°C are seen, although these are quantitatively much less severe (Fig. 8, B and E). TEM analysis of *shi¹* photoreceptors from flies grown at 23°C also showed a variable degree of defects, including poorly formed rhabdomeres (Fig. 8 A, r) and mild accumulations of tubulovesicular intermediates in the cell body (Fig. 8 D, v). However, when *Pld* is overexpressed in *shi¹* photoreceptors at 23°C, the defects in rhabdomere biogenesis are not suppressed (Fig. 8, compare B with C), suggesting that reduced dynamin activity fails to block the effects of elevated PA levels.

The effects of *Pld* overexpression require the activity of type I PIPkin

The activity of type I PI 4 phosphate 5 kinase (PIPkin), a key enzyme in the synthesis of cellular PI 4,5 bisphosphate (PI(4,5)P₂), is known to be regulated by PA (Jenkins et al., 1994). To test whether type I PIPkin activity is required to mediate the effects of PA on transport in photoreceptors, we used a severe hypomorph in *sktl* (*skittles*), one of the two type I PIPkin genes encoded in the *Drosophila* genome (Hassan et al., 1998). Although
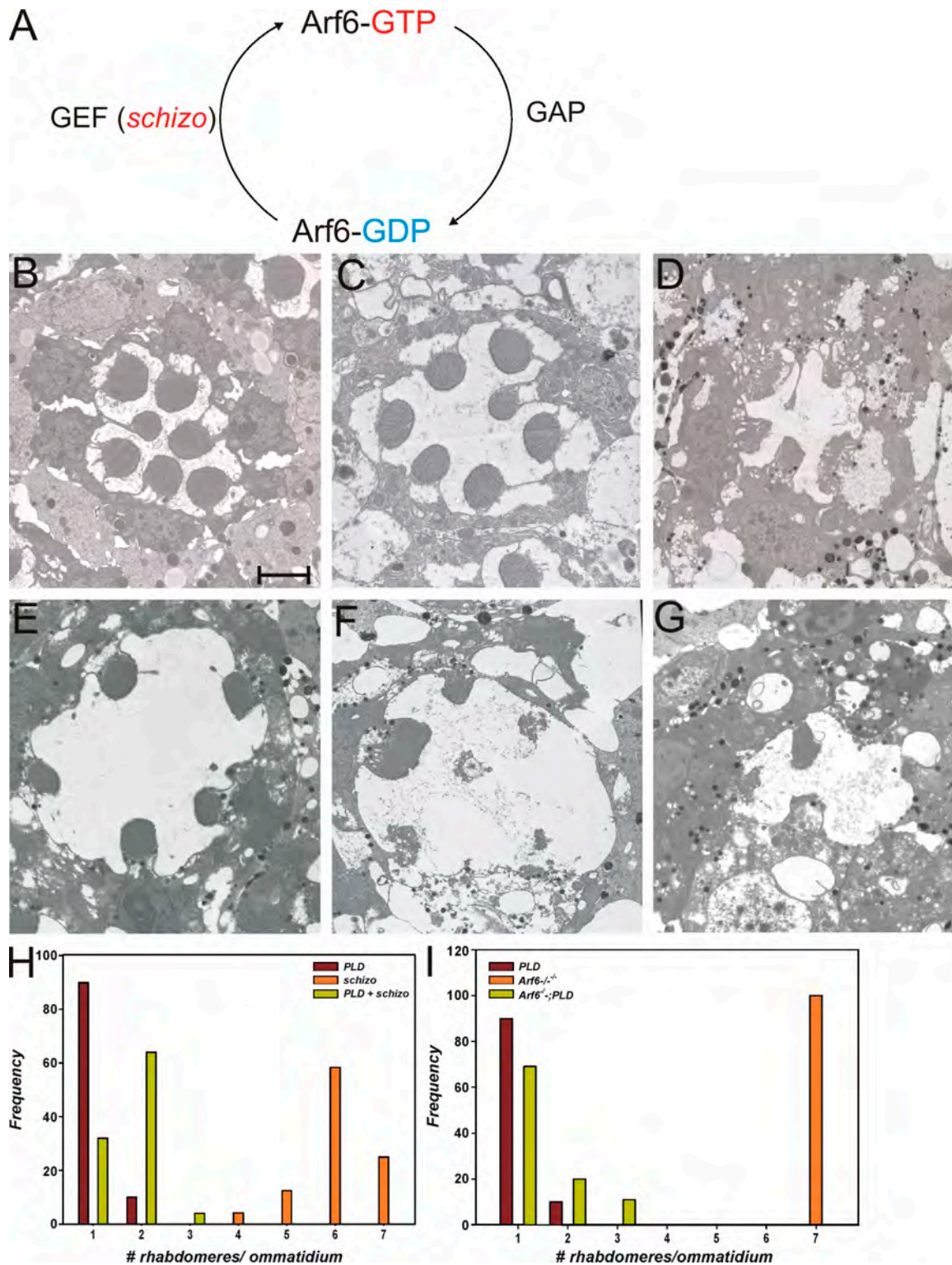
Figure 7. **Effects of *Pld* overexpression in photoreceptors with altered Arf6 activity.** (A) Representation of the activity states of Arf6 and the enzymes that convert Arf6 between these states. Arf6-GTP, GTP-bound Arf6; Arf1-GDP, GDP-bound Arf6. (B–D) TEM analysis of photoreceptors from wild-type (B), Arf6$^{-/-}$ (C), and overexpressing *Pld* in Arf6$^{-/-}$ (D). (E–G) Overexpressing *schizo* alone (E), *Pld* alone (F), and *schizo + Pld* (G). (H and I) Quantitative analysis of rhabdomere biogenesis defects in the aforementioned genotypes. Bar, 2 µm.

the *sktl* gene product is essential for eye development and null mutants in this gene are cell lethal for photoreceptors (Hassan et al., 1998), the *sktl*^{Δ20}/*sktl*$^{Δ1-1}$ allelic combination (that has <5% *sktl* RNA by quantitative PCR analysis) develops viable photoreceptors

that appear normal (Fig. 9 B; Garcia-Murillas et al., 2006). We overexpressed *Pld* in *sktl*^{Δ20}/*sktl*$^{Δ1-1}$ photoreceptors; this revealed a dramatic increase in rhabdomere size compared with photoreceptors overexpressing *Pld* alone (Fig. 9, compare C with D).
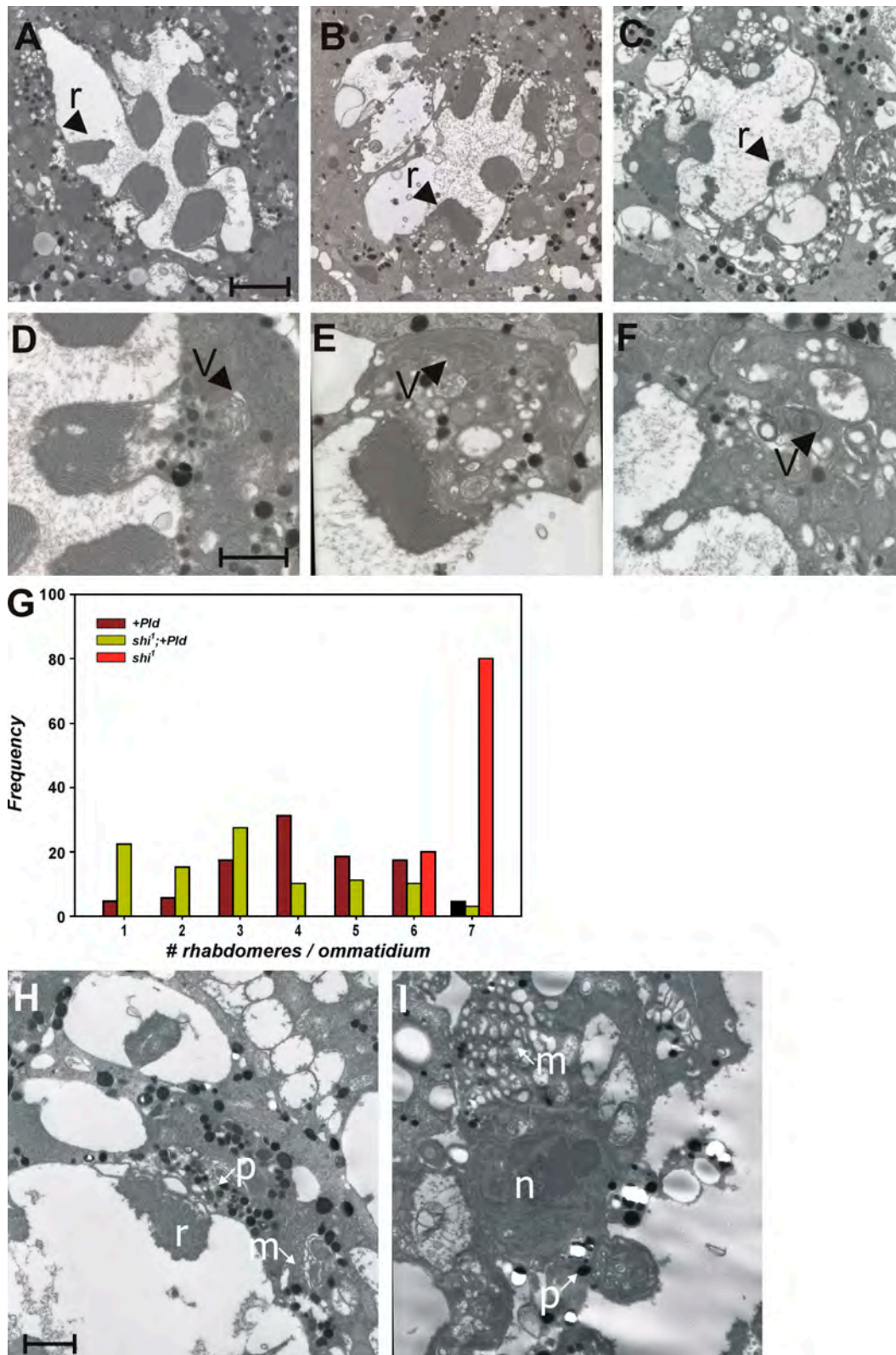
Figure 8. **Effect of overexpressing *Pld* in *shi* mutants.** TEM analysis of an ommatidium from *shi¹* (A) *Pld* overexpression (B) and overexpression of *Pld* in *shi¹* (C). Rhabdomeres (r) are marked. (D–F) Higher magnification views of the rhabdomere and cell body from a single photoreceptor showing tubulovesicular membranes in the cell body (V). (G) Quantitative analysis of rhabdomere biogenesis defects. (H) TEM analysis of photoreceptors from GMR-GAL4* UAS-RNAi^α-adaptin in an otherwise wild-type background. Individual rhabdomeres are smaller and ill formed. The cell bodies show the accumulation of membranous structures (m). (I) Overexpression of UAS-RNAi^α-adaptin and UAS-*Pld* using GMR-GAL4. The nucleus (n) and the pigment granules (p) normally found at the base of the rhabdomeres are marked. A representative example is shown with virtually no detectable rhabdomeres. The cell bodies of the photoreceptors from such animals continued to show accumulation of membrane transport-like intermediates. Bars: (A) 2 μm; (D and H) 1 μm.
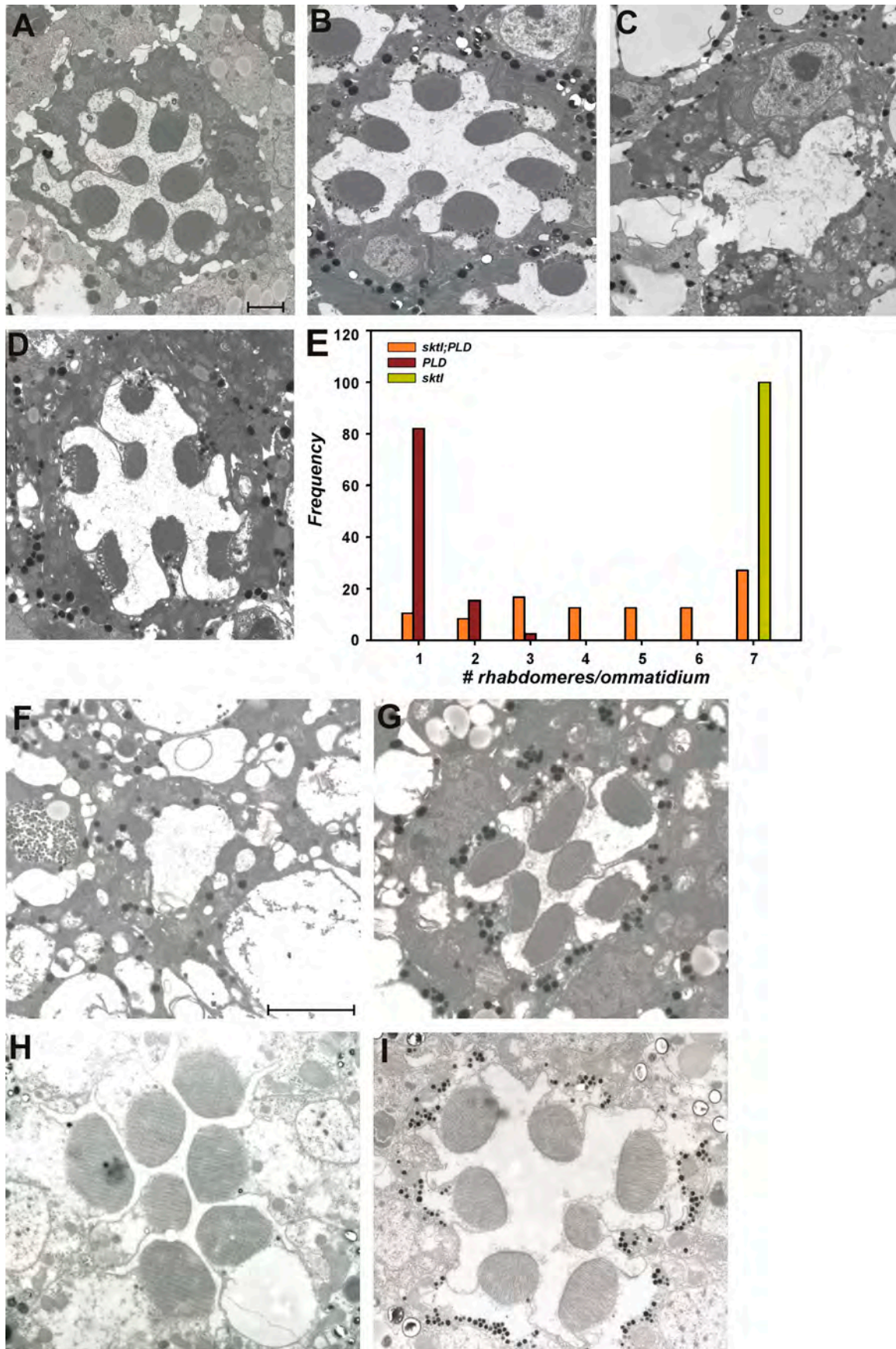
Figure 9. ***sktl* mutants suppress the effects of increased *Pld* activity TEM analysis of photoreceptors.** (A–D) Wild-type (A), *sktl*[Δ20]/*sktl*[Δ1-1] (B), *Pld* alone (C), and *Pld* in a *sktl*[Δ20]/*sktl*[Δ1-1] background (D) are shown. (E) Quantitation of rhabdomere biogenesis defects. Genotypes are marked. The x axis shows bins
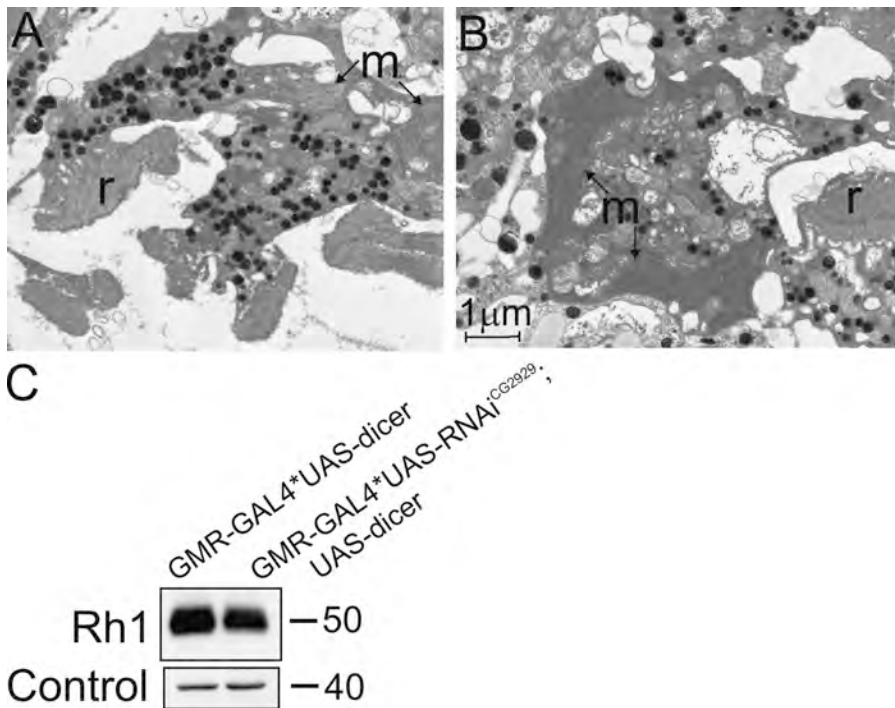
Figure 10. **Effect of RNAi knockdown of PI4K on photoreceptor ultrastructure.** (A and B) TEM analysis showing poorly formed and fragmented rhabdomeres (r). The cell bodies of these photoreceptors show the accumulation of membrane transport intermediates (m). (C) Rh1 protein levels are reduced after RNAi-mediated knockdown of this gene. A loading control band is shown. Unit of measure, M_r.

This finding strongly suggests a requirement for type I PIPkin activity in generating the endomembrane defects observed in photoreceptors with elevated PA levels. An immediate prediction of this observation is that overexpression of *sktl* in developing photoreceptors might also affect rhabdomere biogenesis. We tested this idea by overexpressing *sktl* in developing photoreceptors and compared its effect to that of expressing a point mutant shown to abolish the catalytic activity (kinase-dead *sktl*) of this enzyme (Ishihara et al., 1998). This study revealed that overexpression of wild-type *sktl* resulted in an almost complete block in rhabdomere biogenesis; in contrast, overexpression of kinase-dead *sktl* did not result in this phenotype (Fig. 9, compare F with G). The effects of elevating PA levels by *Pld* overexpression required the enzyme to be present before the onset of rhabdomere biogenesis (Fig. 4). If these effects are mediated by enhanced *sktl* activity, one might predict that the effects of *sktl* overexpression on rhabdomere biogenesis might also only work before this critical time window. To test this idea, we overexpressed *sktl* using Rh1-GAL4 and found that in contrast to overexpression using GMR-GAL4, there was no effect on rhabdomere biogenesis (Fig. 9, compare F with H). These findings suggest that enhanced type I PIPkin activity mediates the effects of elevated PA levels in developing photoreceptors.

Reduction in type II PI 4 kinase (PI4K) levels phenocopy effects of *Pld* overexpression

Work in mammalian cell culture models has suggested that the activity of a PI4K enzyme generating a Golgi localized pool of PI(4)P is important for regulating TGN exit (Godi et al., 1999). To test whether the activity of a PI(4)P-generating enzyme might be critical for rhabdomere biogenesis, we tested the effect of down-regulating PI4K activity in developing photoreceptors. We tested the effect of down-regulating two genes that could encode PI4K activity: CG2929 (PI4KIIβ) and CG10260 (PI4KIIIα). This analysis revealed that down-regulation of CG2929 using RNAi phenocopied key aspects of the phenotype of *Pld* overexpression: (a) down-regulation in the levels of Rh1 protein (Fig. 10 C), (b) formation of small and deformed rhabdomere (Fig. 10 A), and (c) accumulation of abnormal endomembranes within the cell body (Fig. 10 B). These findings suggest that the activity of PI4K is important for membrane transport.

Discussion

PA is a phospholipid that could function during membrane biogenesis in a structural or signaling role. In this study, we have elevated PA levels using three independent genetic manipulations (*cds*[1] and *Pld* or *rdgA* overexpression) in which the only common and immediate biochemical outcome is the accumulation of PA. Using EM to directly visualize photoreceptor membranes, we demonstrate that all three genetic manipulations cause defects in endomembrane organization characterized by a reduction in the size of the apical rhabdomere membrane and/or the accumulation of expanded membranous structures in the cell body. These observations, which are consistent with a defect in membrane transport to the apical domain, are highly

for ommatidia with a given number of rhabdomeres developed. The y axis shows the frequency of rhabdomeres falling within a given bin for each of the genotypes. (F–I) Overexpression of *sktl* in developing photoreceptors is shown. (F and G) TEM images of a single ommatidium from a fly expressing wild-type (F) and kinase-dead (G) *sktl* using GMR-GAL4. A massive block in rhabdomere biogenesis is seen when the wild-type transgene is expressed. (H and I) In contrast, when an Rh1-GAL4 driver is used to express wild-type (H) or kinase-dead (I) *sktl*, no defect in rhabdomere biogenesis is seen. Bars, 2 μm.

reminiscent of defects seen in photoreceptors from *Drosophila* p47 (Sang and Ready, 2002) and Rab11 (Satoh et al., 2005) mutants. Importantly, we also demonstrate that in all three genotypes used to modulate PA levels, the abundance of a single molecular species of PA (16:0/18:2) was elevated without changes in the mass of structural lipids such as PC or of signaling lipids such as PI and DAG. Because this species of PA accounts for <10% of the total PA in photoreceptors, we hypothesize that it represents a quantitatively minor phospholipid that functions in a signaling capacity to modulate membrane transport. The importance of PA for the described phenotypes is supported by the observation that overexpression of a type II PA phosphatase is able to partially revert the defects in rhabdomere biogenesis and endomembrane structure. Together, our findings provide compelling evidence that PA can affect the transport and organization of endomembranes in metazoan cells.

Interestingly, although *cds[1]*, *Pld*, and *rdgA* overexpression all caused endomembrane defects in photoreceptors, the ultrastructural features of the abnormal transport intermediates were variable. All three genotypes showed variable degrees of defect in rhabdomere biogenesis. In addition, in the case of *cds[1]*, the accumulated endomembranes in the cell body resembled ER-like structures (Fig. 2 C); with *Pld* overexpression, there were concentric and sheetlike tubular membranes (Fig. 2 G), whereas with *rdgA* overexpression, in addition to tubular membranes, there were several vesicular intermediates that accumulated (Fig. 2 H). It is likely that these differences reflect the distinct subcellular locations at which PA accumulates in each genotype. In *cds[1]*, PA probably accumulates in the ER site at which CDP-DAG synthase activity is normally present; PLD localization is limited to a compartment at the base of the rhabdomeres, and when overexpressed, DGK is distributed in punctate fashion throughout the ER (unpublished data). The generation of a suitable probe to visualize PA levels in a spatial dimension will be required to address this issue.

During development, the precursor cells of the *Drosophila* eye undergo a substantial increase in size with the concomitant requirement for generating new plasma membrane (Longley and Ready, 1995). During the last 30% of pd, photoreceptors show an approximately fourfold increase in plasma membrane surface area (Raghu et al., 2000), a process that requires a massive surge in polarized membrane transport capacity starting at ∼70% pd. In this study, we have defined a critical time window ∼70% pd before which elevation of PA levels by overexpressing *Pld* results in the endomembrane defects. As this window precedes the onset of rapid membrane transport accompanying rhabdomere biogenesis, we postulate that PA regulates the activity of a component of the molecular machinery that mediates polarized membrane transport during this period. Conceptually, in this respect our findings are reminiscent of observations in the yeast Spo14 mutant, in which membrane transport defects are evident only during the generation of the prospore membrane. To our knowledge, these findings are the first report of regulation of polarized membrane transport by PA in metazoans.

PA affects Arf1-dependent transport

During this study, we observed that the effects of elevated PA (through both *cds[1]* and *Pld* overexpression) were sensitive to the activation state of Arf1. In the *cds[1]* mutant, in which PA is likely to be elevated in the ER, overexpression of the Arf1-GEF *garz* resulted in significantly less developed apical rhabdomere membrane (Fig. 6 B) but was not associated with enhanced accumulation of membranes in the cell body, which is consistent with the known effects of expressing constitutively active Arf1 in cells (Dascher and Balch, 1994). In contrast, overexpression of dArf1-GAP resulted in an enhancement of defective rhabdomere biogenesis as well as a massive accumulation of ER membrane–like intermediates in the cell body (Fig. 6 D). This observation suggests that the PA accumulating at the ER in *cds[1]* influences the Arf1 cycle in this setting, resulting in the transport defects described. Previous biochemical analysis has shown that the activity of Arf1-GAP proteins can be regulated by at least three different lipids relevant to this study, namely PC, DAG (Antonny et al., 1997), and PA (Yanagisawa et al., 2002). In our lipidomic analysis of *cds[1]* retinae, we found that the levels of 34:2 DAG and 34:2 PC were no different from wild type (Fig. 3 D), whereas levels of 34:2 PA were elevated. On the basis of these findings, it is likely that the 34:2 PA that accumulates in *cds[1]* photoreceptors causes the transport defects we have described by down-regulating the activity of Arf1 via dArf1-GAP.

The development and maintenance of apical membranes in polarized cells requires both sorting at the TGN with exocytic transport as well as endocytosis (Bomsel et al., 1989). Thus, the phenotypes resulting from PLD overexpression could be a result of (a) altered membrane transport along one of the steps in the secretory pathway from the ER to the developing rhabdomere or (b) the consequence of enhanced endocytosis from the rhabdomere into the cell body.

Experimental evidence presented in this study shows that in photoreceptors overexpressing *Pld*, the defect in rhabdomere biogenesis was dependent on the levels of active Arf1. In contrast, we found that (a) altering the activity of Arf6, (b) down-regulation of α-adaptin, and (c) a reduction in the function of dynamin (*shi*) did not suppress the effects of overexpressing *Pld*. Collectively, these three observations strongly suggest that excessive clathrin-mediated endocytosis of rhabdomeral plasma membrane does not underlie the endomembrane defects resulting from *Pld* overexpression. A recent study has suggested a role for Arf1 in regulating a dynamin-independent endocytic pathway in *Drosophila* cells (Kumari and Mayor, 2008). The role of this pathway in the effects of *Pld* overexpression remains unknown.

Arf1 also exerts several effects on distinct steps of the exocytic pathway, including bidirectional transport between the ER and Golgi (Lee et al., 2004) between Golgi cisternae and the regulation of exit from the late Golgi (D'Souza-Schorey and Chavrier, 2006). In photoreceptors overexpressing *Pld*, our analysis suggests that ER to trans-Golgi transport was normal (Fig. S2), implying that the observed phenotypes are likely to involve a transport step between the TGN and plasma membrane, although observed phenotypes do not phenocopy exocyst loss of function (Fig. S3). In *Drosophila* photoreceptors, PLD localizes to a restricted subcompartment at the base of the rhabdomeres (Fig. S5 A). Although the molecular identity of this compartment has not been established, its subcellular localization is consistent with the ability of PA produced by PLD to regulate transport between the rhabdomeres and cell body. In TEMs of photoreceptors overexpressing

Pld, the endomembranes we observed in the cell body showed a tubulovesicular morphology extending throughout the cytoplasm (e.g., Fig. 2 E). These membranes resemble large pleiomorphic carriers (Polishchuk et al., 2000; Luini et al., 2005), transport intermediates that derive from the TGN destined for acceptor compartments like the plasma membrane. Furthermore, vesicles containing proteins destined for and normally restricted to the apical rhabdomere membrane (such as Rh1) are found in the cell body of photoreceptors overexpressing *Pld* (Fig. 4 F). These observations are particularly interesting in the light of previous studies suggesting that PA generated by PLD can regulate the release of vesicles from the Golgi in an Arf1-dependent manner (Ktistakis et al., 1996; Chen et al., 1997). However, in the absence of a clear identification of the accumulated membranes, the precise definition of the affected transport intermediates we have observed remains elusive.

Arf1 can influence several events at the TGN (for review see De Matteis and Luini, 2008), including the recruitment and activation of phospholipid-metabolizing enzymes. These include the recruitment and activation of PI4KIIIβ (Godi et al., 1999) generating PI(4)P as well a direct role in activating the type I PIPkin on Golgi membranes in vitro (Jones et al., 2000). During this study, we found that (a) down-regulating the levels of a PI4K expressed during photoreceptor development phenocopies key aspects of that seen with *Pld* overexpression (Fig. 10), and (b) a strong hypomorph of the type I PIPkin (*sktl*) was able to substantially suppress the effects of *Pld* overexpression on rhabdomere biogenesis. These observations reflect the importance of tightly regulating type I PIPkin activity by PA for normal transport to the apical domain in polarized cells. They suggest that the regulation of PI(4)P levels is critical for rhabdomere biogenesis. In the context of interpreting the effects of *Pld* overexpression, it is possible that raised PA levels lead to enhanced activity of type I PIPkin consuming PI(4)P at the TGN, resulting in consequent transport defects to the apical membrane. Although we have not been able to demonstrate reduced PI(4)P or increased $PI(4,5)P_2$ levels at the Golgi in photoreceptors overexpressing *Pld*, our observation that overexpression of *sktl* in developing photoreceptors before the critical time window (but not a kinase-dead version) results in a massive defect in rhabdomere biogenesis underscores the importance of tight regulation of type I PIPkin activity during this process. Thus, a tight regulation of the balance of PI(4)P and $PI(4,5)P_2$ levels through Arf1 activity may underlie the effects of PA in this system.

Given the large number of effectors that can be regulated by PA (Stace and Ktistakis, 2006), in the future, it will be important to identify and understand the functions of those that play a role in the biogenesis of rhabdomeres during photoreceptor development.

Materials and methods

Fly culture and stocks
Flies (*Drosophila*) were reared on standard cornmeal, dextrose, and yeast medium at 25°C and 50% relative humidity in a constant temperature laboratory incubator. When required, temperature-sensitive mutants such as *shi* and *ninaA* were grown in separate incubators set to the appropriate temperature. There was no internal illumination within the incubator, and flies were only subject to brief pulses of light when the incubator door was opened. When required, flies were grown in a cooled incubator with constant illumination from a white light source. For experiments involving dark rearing, flies were grown in vials kept in tightly closed black photographic bags inside a cooled incubator maintained at 25°C.

EM
Eyes were prepared for histology by dissecting in ice-cold fixative (2% formaldehyde and 2.5% glutaraldehyde in 0.1 M Na cacodylate buffer, pH 7.3). After 4 h fixation at 4°C, eyes were buffer washed, postfixed in 1% OsO_4 for 1 h, and stained en bloc in uranyl acetate for 1 h. Eyes were dehydrated in an alcohol series and embedded in Spurr's. 70-nm ultrathin sections were stained with uranyl acetate and lead citrate and viewed on a transmission electron microscope (CM100; Phillips).

Generation of *Pld* overexpression flies
The *Pld* cDNA used in this study originated from the clone pOT2a-GH07346 generated by the Berkeley *Drosophila* Genome Project. This clone has been fully sequenced by the Berkeley *Drosophila* Genome Project, and its sequence is available in GenBank (accession no. AF145640). Overexpression in the retina was perfomed using the modular GAL4-UAS system. To generate transgenic flies, the *Pld* open reading frame was subcloned into the EcoRI and NotI sites of pUAST (Brand and Perrimon, 1993). To generate a catalytically dead *Pld* (the K1086R mutation; Fig. S2), the wild-type gene was subcloned into pBluescript using EcoRI and NotI, and the mutation was introduced by standard site-directed mutagenesis. After sequencing, the K/R *Pld* was subcloned into the germline transformation vector pUAST using EcoRI/NotI. Germline transformation was performed using established protocols. w^{1118} embryos were injected, and several independent transgenic lines were obtained. They were mapped using standard genetic crosses to obtain stocks carrying single mapped insertions. Such stocks were used in the experiments described in this study.

Immunohistochemistry
Whole-mount immunohistochemistry was performed using a modification of previously published methods (Karagiosis and Ready, 2004). Retinae were dissected in ice-cold PBS and fixed with 4% paraformaldehyde in PBS for 1 h on ice. Fixed eyes were given three 10-min washes in PBST (PBS with 0.25% Triton X-100). Blocking was performed using 10% FBS for 1 h at room temperature. Incubations with primary antibodies (diluted in PBST with 5% FBS) were performed at 4°C overnight. After washes in PBST, samples were incubated in secondary antibodies diluted in PBST for 2 h at room temperature. Samples were washed in PBST and mounted in Citifluor (Agar Scientific). Samples were viewed using a confocal microscope (LSM 510 META; Carl Zeiss, Inc.) using either a Plan-Neofluar 40× NA 1.30 or a Plan-Apochromat 63× NA 1.40 oil objective (Carl Zeiss, Inc.).

Isolation of pure retinal tissue
Pure preparations of retinal tissue were collected using previously described methods (Garcia-Murillas et al., 2006). In brief, flies were snap frozen in liquid nitrogen and dehydrated in acetone at −20°C for 48 h. The acetone was drained off, and the retinae dried at room temperature. They were cleanly separated from the head at the level of the basement membrane using a flattened insect pin. This allows the preparation of a largely pure collection of retinae.

Heat shock expression experiments
Wandering third instar larvae were collected at pupariation (0% pd) and aged at 25°C on a moist Whatman paper in a Petri dish in a cooled incubator. Under these conditions, in our hands, adult flies eclosed at 100 h. Pupae from this collection were removed and subjected to a 1-h heat shock at 37°C in a water bath. After this, they were transferred into a vial with normal culture medium and allowed to complete development in the vial until adult flies emerged. 0–12-h-old flies were separated into non-expressing controls and *Pld*-expressing animals (flies with curly or straight wings, respectively). They were decapitated using a sharp razor blade, and protein extracts were prepared from the heads as described in Western blot analysis.

Western blot analysis
Protein analysis was performed with flies aged 0–12 h posteclosion. Heads were prepared by decapitating flies cooled on ice. Where specified, the samples used were dissected freeze-dried retinae. Samples were homogenized in 2× SDS-PAGE sample buffer followed by boiling at 100°C for 1 min. Samples were separated using SDS-PAGE and electroblotted onto supported nitrocellulose membrane (Hybond-C extra; GE Healthcare) using wet transfer. The uniformity of transfer onto membranes was checked by staining with Ponceau S. After blocking in 5% nonfat milk (Marvel),

blots were incubated for 1 h at room temperature in appropriate dilutions of primary antibody. Immunoreactive protein was visualized after incubation in a 1:10,000 dilution of donkey α–rabbit IgG coupled to horseradish peroxidase (Jackson ImmunoResearch Laboratories) for 1 h at room temperature, and the blots were developed with ECL (GE Healthcare).

Antibodies
The following antibodies were used in this study: antirhodopsin mouse monoclonal 4C5 (Developmental Studies Hybridoma Bank), anti-Golgi mouse monoclonal 7H6D7C2 (EMD), anti-Bip rat monoclonal antibody clone 143 (Babraham Bioscience Technologies), antiwind rabbit polyclonal (provided by D. Ferrari, Max Planck Institute, Gottingen, Germany), anti-syntaxin16 (provided by W. Trimble, University of Toronto, Toronto, Ontario, Canada), anti-PLC (provided by B. Hwa-Shieh, Vanderbilt University, Nashville, TN), anti-TRP (provided by C. Montell, John Hopkins University, Baltimore, MD), and anti-KDEL (provided by G. Butcher, The Babraham Institute, Cambridge, England, UK). For immunofluorescence, anti–mouse Alexa Fluor 488 and anti–rat Alexa Fluor 633 (Invitrogen) were used.

Generation of anti-*Pld* antibody
A fragment of *Pld* encompassing amino acids 607–789 (start, RWDDH-HHRLT; end, GQEVAITTSS) was subcloned into the pGEX vector (GE Healthcare) and expressed as a GST fusion protein in *Escherichia coli* BL-21 cells. After purification of this fragment using standard procedures, ~3 mg total protein was injected into rabbits to produce polyclonal antibodies. Highest titers were obtained from the final bleed, and most experiments shown have used this serum. In some experiments, antibodies were affinity purified as follows: 2 ml total serum was incubated with beads coupled to GST, and nonbound material was collected. This material was incubated with beads coupled to GST-PLD, and bound material was eluted with glycine, pH 2.5. After neutralization, the purified antibodies were aliquoted and stored at −20°C until use.

Analysis of retinal lipids
150 freeze-dried retinae (dissected as described in Isolation of pure retinal tissue) were homogenized in 0.5 ml methanol (containing 500 ng each of 12:0/12:0 species of DAG, PA, PC, phosphatidylethanol, PG, and PS as internal standards) using a 1-ml glass homogenizer until completely disrupted (>100 strokes). The methanolic homogenate was transferred into a glass screw-capped tube. Further methanol (0.5 ml) was used to wash the homogenizer and was combined in the glass tube. 2 ml chloroform was added and left to stand for 10 min. 0.88% KCl (1 ml) was added to split the phases. After removal of the upper phase and interfacial material, the lower organic phase containing the lipids was dried, resuspended in 15 µl chloroform, and finally transferred into a silanized autosampler vial ready for analysis.

Phospholipids (1-µl injection) were separated on a 1.0 × 150–mm silica column (3 µm, Luna; Phenomenex) using 100% chloroform/methanol/water (90:9.5:0.5) containing 7.5 mM ethylamine changing to 100% acetonitrile/chloroform/methanol/water (30:30:35:5) containing 10 mM ethylamine over 20 min at 100 µl/min. Detection was performed by electrospray ionization in both positive (PC) and negative modes (PA, phosphatidylethanol, PG, PI, and PS) on a single quadruple mass spectrometer (probe voltage, ±4 kV; nebulizer gas, 4 liters/min N_2; desolvation line temperature, 300°C; QP8000α; Shimadzu). Subsequent lipid analysis adopted a similar chromatographic separation but analyzed the lipid structures in a semiquantitative manner using a mass spectrometer (LCMS-IT-TOF; Shimadzu). The detection methodology of this machine has a considerably greater sensitivity and mass accuracy; consequently, the data in Fig. 3 (compare A and B with C) are qualitatively similar but slightly different quantitatively. In all graphs, the control and experimental data presented have been gathered on the same machine.

Generation of stable *Pld*-expressing S2 cell lines
The gene for *Pld* was subcloned using EcoRI/NotI into vector pCMV3-myc, which introduces a myc tag at the N terminus. The myc-*Pld* construct was subsequently subcloned into pRmHa-3 using Kpn1. The pRmHa-3-*Pld* vector was transfected into S2 cells using Fugene (Roche), and stable cell lines were selected after growth of resistant cells in 0.5 mg/ml of G418. In these cells, expression of *Pld* is inducible using $CuSO_4$ (usually 500–700 µM overnight). A similar strategy was used to derive S2 cells expressing the *Pld*-K1086R catalytically inactive mutant.

Biochemical analysis of PLD activity
Measurement of PLD activity was done in stable S2 cells expressing *Pld* or in COS-7 cells transfected with myc-tagged *Pld* or the K1086R mutant. In all cases, cells in 6-well plates were labeled overnight in 1% dialyzed serum containing 300 µCi per well of ^3H palmitic acid. The following morning, the medium was made to contain 1% butanol (as indicated) for 30 min, and the cells were collected and extracted for lipid analysis as described previously (Manifava et al., 1999).

References

Alloway, P.G., L. Howard, and P.J. Dolph. 2000. The formation of stable rhodopsin-arrestin complexes induces apoptosis and photoreceptor cell degeneration. *Neuron.* 28:129–138.

Antonny, B., I. Huber, S. Paris, M. Chabre, and D. Cassel. 1997. Activation of ADP-ribosylation factor 1 GTPase-activating protein by phosphatidylcholine-derived diacylglycerols. *J. Biol. Chem.* 272:30848–30851.

Bankaitis, V.A., J.R. Aitken, A.E. Cleves, and W. Dowhan. 1990. An essential role for a phospholipid transfer protein in yeast Golgi function. *Nature.* 347:561–562.

Bomsel, M., K. Prydz, R.G. Parton, J. Gruenberg, and K. Simons. 1989. Endocytosis in filter-grown Madin-Darby canine kidney cells. *J. Cell Biol.* 109:3243–3258.

Brand, A.H., and N. Perrimono. 1993. Targeted gene expression as a means of altering cell fates and generating dominant phenotypes. *Development.* 118:401–415.

Brown, H.A., S. Gutowski, C.R. Moomaw, C. Slaughter, and P.C. Sternweis. 1993. ADP-ribosylation factor, a small GTP-dependent regulatory protein, stimulates phospholipase D activity. *Cell.* 75:1137–1144.

Cai, D., M. Zhong, R. Wang, W.J. Netzer, D. Shields, H. Zheng, S.S. Sisodia, D.A. Foster, F.S. Gorelick, H. Xu, and P. Greengard. 2006. Phospholipase D1 corrects impaired betaAPP trafficking and neurite outgrowth in familial Alzheimer's disease-linked presenilin-1 mutant neurons. *Proc. Natl. Acad. Sci. USA.* 103:1936–1940.

Chen, Y.G., A. Siddhanta, C.D. Austin, S.M. Hammond, T.C. Sung, M.A. Frohman, A.J. Morris, and D. Shields. 1997. Phospholipase D stimulates release of nascent secretory vesicles from the *trans*-Golgi network. *J. Cell Biol.* 138:495–504.

Choi, W.S., Y.M. Kim, C. Combs, M.A. Frohman, and M.A. Beaven. 2002. Phospholipases D1 and D2 regulate different phases of exocytosis in mast cells. *J. Immunol.* 168:5682–5689.

Cleves, A.E., T.P. McGee, E.A. Whitters, K.M. Champion, J.R. Aitken, W. Dowhan, M. Goebl, and V.A. Bankaitis. 1991. Mutations in the CDP-choline pathway for phospholipid biosynthesis bypass the requirement for an essential phospholipid transfer protein. *Cell.* 64:789–800.

Cockcroft, S., G.M. Thomas, A. Fensome, B. Geny, E. Cunningham, I. Gout, I. Hiles, N.F. Totty, O. Truong, and J.J. Hsuan. 1994. Phospholipase D: a downstream effector of ARF in granulocytes. *Science.* 263:523–526.

Cockcroft, S., G. Way, N. O'Luanaigh, R. Pardo, E. Sarri, and A. Fensome. 2002. Signalling role for ARF and phospholipase D in mast cell exocytosis stimulated by crosslinking of the high affinity FcepsilonR1 receptor. *Mol. Immunol.* 38:1277–1282.

Cox, R., R.J. Mason-Gamer, C.L. Jackson, and N. Segev. 2004. Phylogenetic analysis of Sec7-domain-containing Arf nucleotide exchangers. *Mol. Biol. Cell.* 15:1487–1505.

D'Souza-Schorey, C., and P. Chavrier. 2006. ARF proteins: roles in membrane traffic and beyond. *Nat. Rev. Mol. Cell Biol.* 7:347–358.

Dascher, C., and W.E. Balch. 1994. Dominant inhibitory mutants of ARF1 block endoplasmic reticulum to Golgi transport and trigger disassembly of the Golgi apparatus. *J. Biol. Chem.* 269:1437–1448.

De Matteis, M.A., and A. Luini. 2008. Exiting the Golgi complex. *Nat. Rev. Mol. Cell Biol.* 9:273–284.

Dietzl, G., D. Chen, F. Schnorrer, K.C. Su, Y. Barinova, M. Fellner, B. Gasser, K. Kinsey, S. Oppel, S. Scheiblauer, et al. 2007. A genome-wide transgenic RNAi library for conditional gene inactivation in *Drosophila*. *Nature*. 448:151–156.

Franco, M., P.J. Peters, J. Boretto, E. van Donselaar, A. Neri, C. D'Souza-Schorey, and P. Chavrier. 1999. EFA6, a sec7 domain-containing exchange factor for ARF6, coordinates membrane recycling and actin cytoskeleton organization. *EMBO J.* 18:1480–1491.

Frolov, M.V., and V.E. Alatortsev. 2001. Molecular analysis of novel *Drosophila* gene, Gap69C, encoding a homolog of ADP-ribosylation factor GTPase-activating protein. *DNA Cell Biol.* 20:107–113.

Garcia-Murillas, I., T. Pettitt, E. Macdonald, H. Okkenhaug, P. Georgiev, D. Trivedi, B. Hassan, M. Wakelam, and P. Raghu. 2006. lazaro encodes a lipid phosphate phosphohydrolase that regulates phosphatidylinositol turnover during *Drosophila* phototransduction. *Neuron.* 49:533–546.

Gillingham, A.K., and S. Munro. 2007. The small G proteins of the Arf family and their regulators. *Annu. Rev. Cell Dev. Biol.* 23:579–611.

Godi, A., P. Pertile, R. Meyers, P. Marra, G. Di Tullio, C. Iurisci, A. Luini, D. Corda, and M.A. De Matteis. 1999. ARF mediates recruitment of PtdIns-4-OH kinase-beta and stimulates synthesis of PtdIns(4,5)P2 on the Golgi complex. *Nat. Cell Biol.* 1:280–287.

Gonzalez-Gaitan, M., and H. Jackle. 1997. Role of *Drosophila* alpha-adaptin in presynaptic vesicle recycling. *Cell.* 88:767–776.

Hardie, R.C., and B. Minke. 1992. The Trp gene is essential for a light-activated Ca2+ channel in *Drosophila* photoreceptors. *Neuron.* 8:643–651.

Hardie, R.C., and P. Raghu. 2001. Visual transduction in *Drosophila*. *Nature.* 413:186–193.

Hassan, B.A., S.N. Prokopenko, S. Breuer, B. Zhang, A. Paululat, and H.J. Bellen. 1998. skittles, a *Drosophila* phosphatidylinositol 4-phosphate 5-kinase, is required for cell viability, germline development and bristle morphology, but not for neurotransmitter release. *Genetics.* 150:1527–1537.

Heacock, A.M., and B.W. Agranoff. 1997. CDP-diacylglycerol synthase from mammalian tissues. *Biochim. Biophys. Acta.* 1348:166–172.

Huang, P., Y.M. Altshuller, J.C. Hou, J.E. Pessin, and M.A. Frohman. 2005. Insulin-stimulated plasma membrane fusion of Glut4 glucose transporter-containing vesicles is regulated by phospholipase D1. *Mol. Biol. Cell.* 16:2614–2623.

Ishihara, H., Y. Shibasaki, N. Kizuki, T. Wada, Y. Yazaki, T. Asano, and Y. Oka. 1998. Type I phosphatidylinositol-4-phosphate 5-kinases. Cloning of the third isoform and deletion/substitution analysis of members of this novel lipid kinase family. *J. Biol. Chem.* 273:8741–8748.

Jenkins, G.H., P.L. Fisette, and R.A. Anderson. 1994. Type I phosphatidylinositol 4-phosphate 5-kinase isoforms are specifically stimulated by phosphatidic acid. *J. Biol. Chem.* 269:11547–11554.

Jones, D.H., J.B. Morris, C.P. Morgan, H. Kondo, R.F. Irvine, and S. Cockcroft. 2000. Type I phosphatidylinositol 4-phosphate 5-kinase directly interacts with ADP-ribosylation factor 1 and is responsible for phosphatidylinositol 4,5-bisphosphate synthesis in the golgi compartment. *J. Biol. Chem.* 275:13962–13966.

Kiselev, A., M. Socolich, J. Vinos, R.W. Hardy, C.S. Zuker, and R. Ranganathan. 2000. A molecular pathway for light-dependent photorecptor apoptosis in *Drosophila*. *Neuron.* 28:139–152.

Kosaka, T., and K. Ikeda. 1983. Possible temperature-dependent blockage of synaptic vesicle recycling induced by a single gene mutation in *Drosophila*. *J. Neurobiol.* 14:207–225.

Kraut, R., K. Menon, and K. Zinn. 2001. A gain-of-function screen for genes controlling motor axon guidance and synaptogenesis in *Drosophila*. *Curr. Biol.* 11:417–430.

Ktistakis, N.T., H.A. Brown, M.G. Waters, P.C. Sternweis, and M.G. Roth. 1996. Evidence that phospholipase D mediates ADP ribosylation factor-dependent formation Golgi coated vesicles. *J. Cell Biol.* 134:295–306.

Kumari, S., and S. Mayor. 2008. ARF1 is directly involved in dynamin-independent endocytosis. *Nat. Cell Biol.* 10:30–41.

Lalonde, M.M., H. Janssens, E. Rosenbaum, S.Y. Choi, J.P. Gergen, N.J. Colley, W.S. Stark, and M.A. Frohman. 2005. Regulation of phototransduction responsiveness and retinal degeneration by a phospholipase D–generated signaling lipid. *J. Cell Biol.* 169:471–479.

Lee, M.C., E.A. Miller, J. Goldberg, L. Orci, and R. Schekman. 2004. Bi-directional protein transport between the ER and Golgi. *Annu. Rev. Cell Dev. Biol.* 20:87–123.

Leonard, D.S., V.D. Bowman, D.F. Ready, and W.L. Pak. 1992. Degeneration of photoreceptors in rhodopsin mutants of *Drosophila*. *J. Neurobiol.* 23:605–626.

Longley, R.L. Jr., and D.F. Ready. 1995. Integrins and the development of three-dimensional structure in the *Drosophila* compound eye. *Dev. Biol.* 171:415–433.

Luini, A., A. Ragnini-Wilson, R.S. Polishchuck, and M.A. De Matteis. 2005. Large pleiomorphic traffic intermediates in the secretory pathway. *Curr. Opin. Cell Biol.* 17:353–361.

Manifava, M., J. Sugars, and N.T. Ktistakis. 1999. Modification of catalytically active phospholipase D1 with fatty acid in vivo. *J. Biol. Chem.* 274:1072–1077.

Masai, I., A. Okazaki, T. Hosoya, and Y. Hotta. 1993. *Drosophila* retinal degeneration a-gene encodes an eye-specific diacylglycerol kinase with cysteine-rich zinc-finger motifs and ankyrin repeats. *Proc. Natl. Acad. Sci. USA.* 90:11157–11161.

Montell, C., and G.M. Rubin. 1989. Molecular characterization of the *Drosophila* Trp locus: a putative integral membrane-protein required for phototransduction. *Neuron.* 2:1313–1323.

Nakanishi, H., M. Morishita, C.L. Schwartz, A. Coluccio, J. Engebrecht, and A.M. Neiman. 2006. Phospholipase D and the SNARE Sso1p are necessary for vesicle fusion during sporulation in yeast. *J. Cell Sci.* 119:1406–1415.

Onel, S., L. Bolke, and C. Klambt. 2004. The *Drosophila* ARF6-GEF Schizo controls commissure formation by regulating Slit. *Development.* 131:2587–2594.

Perletti, L., D. Talarico, D. Trecca, D. Ronchetti, N.S. Fracchiolla, A.T. Maiolo, and A. Neri. 1997. Identification of a novel gene, PSD, adjacent to NFKB2/lyt-10, which contains Sec7 and pleckstrin-homology domains. *Genomics.* 46:251–259.

Polishchuk, R.S., E.V. Polishchuk, P. Marra, S. Alberti, R. Buccione, A. Luini, and A.A. Mironov. 2000. Correlative light-electron microscopy reveals the tubular-saccular ultrastructure of carriers operating between Golgi apparatus and plasma membrane. *J. Cell Biol.* 148:45–58.

Raghu, P., K. Usher, S. Jonas, S. Chyb, A. Polyanovsky, and R.C. Hardie. 2000. Constitutive activity of the light-sensitive channels TRP and TRPL in the *Drosophila* diacylglycerol kinase mutant, rdgA. *Neuron.* 26:169–179.

Robinson, M.S. 2004. Adaptable adaptors for coated vesicles. *Trends Cell Biol.* 14:167–174.

Rorth, P. 1996. A modular misexpression screen in *Drosophila* detecting tissue-specific phenotypes. *Proc. Natl. Acad. Sci. USA.* 93:12418–12422.

Rudge, S.A., A.J. Morris, and J. Engebrecht. 1998. Relocalization of phospholipase D activity mediates membrane formation during meiosis. *J. Cell Biol.* 140:81–90.

Rudge, S.A., T.R. Pettitt, C. Zhou, M.J. Wakelam, and J.A. Engebrecht. 2001. SPO14 separation-of-function mutations define unique roles for phospholipase D in secretion and cellular differentiation in *Saccharomyces cerevisiae*. *Genetics.* 158:1431–1444.

Sang, T.-K., and D.F. Ready. 2002. Eyes closed, a *Drosophila* p47 homolog, is essential for photoreceptor morphogenesis. *Development.* 129:143–154.

Satoh, A.K., J.E. O'Tousa, K. Ozaki, and D.F. Ready. 2005. Rab11 mediates post-Golgi trafficking of rhodopsin to the photosensitive apical membrane of *Drosophila* photoreceptors. *Development.* 132:1487–1497.

Schneuwly, S., M.G. Burg, C. Lending, M.H. Perdew, and W.L. Pak. 1991. Properties of photoreceptor-specific phospholipase C encoded by the norpA gene of *Drosophila melanogaster*. *J. Biol. Chem.* 266:24314–24319.

Someya, A., M. Sata, K. Takeda, G. Pacheco-Rodriguez, V.J. Ferrans, J. Moss, and M. Vaughan. 2001. ARF-GEP(100), a guanine nucleotide-exchange protein for ADP-ribosylation factor 6. *Proc. Natl. Acad. Sci. USA.* 98:2413–2418.

Sreenivas, A., J.L. Patton-Vogt, V. Bruno, P. Griac, and S.A. Henry. 1998. A role for phospholipase D (Pld1p) in growth, secretion, and regulation of membrane lipid synthesis in yeast. *J. Biol. Chem.* 273:16635–16638.

Stace, C.L., and N.T. Ktistakis. 2006. Phosphatidic acid- and phosphatidylserine-binding proteins. *Biochim. Biophys. Acta.* 1761:913–926.

van der Bliek, A.M., and E.M. Meyerowitz. 1991. Dynamin-like protein encoded by the *Drosophila* shibire gene associated with vesicular traffic. *Nature.* 351:411–414.

Vitale, N., A.S. Caumont, S. Chasserot-Golaz, G. Du, S. Wu, V.A. Sciorra, A.J. Morris, M.A. Frohman, and F. Bader. 2001. Phospholipase D1: a key factor for the exocytotic machinery in neuroendocrine cells. *EMBO J.* 20:2424–2434.

Wu, L., B. Niemeyer, N. Colley, M. Socolich, and C.S. Zuker. 1995. Regulation of PLC-mediated signalling in vivo by CDP-diacylglycerol synthase. *Nature.* 373:216–222.

Xie, Z., M. Fang, M.P. Rivas, A.J. Faulkner, P.C. Sternweis, J.A. Engebrecht, and V.A. Bankaitis. 1998. Phospholipase D activity is required for suppression of yeast phosphatidylinositol transfer protein defects. *Proc. Natl. Acad. Sci. USA.* 95:12346–12351.

Yanagisawa, L.L., J. Marchena, Z. Xie, X. Li, P.P. Poon, R.A. Singer, G.C. Johnston, P.A. Randazzo, and V.A. Bankaitis. 2002. Activity of specific lipid-regulated ADP ribosylation factor-GTPase-activating proteins is required for Sec14p-dependent Golgi secretory function in yeast. *Mol. Biol. Cell.* 13:2193–2206.